

## Research Note

# Photometric properties of single stellar populations: From $Z/Z_{\odot} = 1/50$ to $Z/Z_{\odot} = 2.5$

M. Mouhcine<sup>1,2</sup> and A. Lançon<sup>1</sup>

<sup>1</sup> Observatoire Astronomique de Strasbourg (UMR 7550), 11 rue de l'Université, 67000 Strasbourg, France

<sup>2</sup> Department of Physics and Astronomy, UCLA, Math-Sciences Building 8979, Los Angeles, CA 90095-1562, USA

Received 31 July 2002 / Accepted 14 January 2003

**Abstract.** We describe a large grid of photometric properties of single stellar populations that focuses on the near infrared properties of intermediate age populations. The underlying model was presented in recent articles, where we compared its predictions with observations of properties of star clusters and of asymptotic giant branch populations of Local Group galaxies. The grid is made available in tabular form. We present the time evolution of optical and near-infrared broadband colours in the *BVIJHK* passbands, with ages ranging from 50 Myr to 15 Gyr, and for initial chemical compositions [ $Z = 0.0004, Y = 0.23$ ], [ $Z = 0.004, Y = 0.24$ ], [ $Z = 0.008, Y = 0.25$ ], [ $Z = 0.02, Y = 0.28$ ], and [ $Z = 0.05, Y = 0.352$ ]. The evolution of the stellar mass-to-light ratio in the *V* and *K* passbands is also provided. All the stellar models are followed from the zero age main sequence (ZAMS) to the central carbon ignition for massive stars, or to the end of the thermally pulsing regime of the asymptotic giant branch phase (TP-AGB) for low and intermediate mass stars. Calculations of other quantities are possible upon request.

**Key words.** stars: AGB and post-AGB – galaxies: star clusters – galaxies: stellar content – galaxies: evolution

## 1. Introduction

Predicting the integrated spectral energy distributions (SEDs) of stellar populations is an important issue in the solution of many problems in astronomy, from determining the properties of star clusters in nearby galaxies and the Milky Way, to modelling the star formation history of galaxies at cosmological distances. A huge amount of spectrophotometric data is already available in the literature, and more will become available in the near future (for instance through the Sloan Digital Sky Survey or the 6dF survey). Synthetic SEDs will be used extensively to achieve the scientific goals of these observational programs.

Colour distributions of star clusters have been observed for large numbers of galaxies with different morphologies (Zepf & Ashman 1993; Schweizer et al. 1996; Forbes et al. 2000; Whitmore et al. 2002). An important issue of modern astrophysics concerns the interpretation of those distributions in relation to the formation histories of their parent galaxies. The determination of ages and metallicities of the star clusters is needed to address such questions. In the quest for large samples of star clusters, the magnitude limits for spectroscopic investigations are rapidly exceeded, and the desired fundamental properties must be determined from broad band colours.

Both for the study of clusters and as simple components of more complex star formation histories, it is necessary to study the evolution of broad band photometric properties of stellar populations formed within a very short timescale, the so-called Single Stellar Populations (SSPs hereafter). It is also necessary to investigate how this evolution is affected by metallicity.

The subject of population synthesis has a long history, and is an active area of research: synthesis techniques and many of the input data (stellar evolutionary tracks, spectral libraries, properties of interstellar medium, etc.) continue to be improved. Successive generations of modelers have combined the best available knowledge on the ingredients of population synthesis models to predict the appearance of the combined light of generations of stars (Tinsley 1980; Bruzual 1983; Arimoto & Yoshii 1987; Charlot & Bruzual 1991; Bertelli et al. 1994; Lançon & Rocca-Volmerange 1996; Fioc & Rocca-Volmerange 1997; Kurth et al. 1999; Leitherer et al. 1999; Girardi et al. 2000). Nevertheless the actual understanding of near-infrared properties has remained a subject of debate, in particular at intermediate ages, between 0.1 and 2–3 Gyr (Girardi & Bertelli 1998; Maraston 1998). The main culprits are the luminous asymptotic giant branch stars (AGB stars). Fundamental difficulties are faced in the accurate modelling of their evolution (convection, rapid structural modifications in thermal pulses, pulsation modes, mass loss)

---

Send offprint requests to: M. Mouhcine,  
e-mail: mouhcine@astro.ucla.edu

and their spectra (non-static extended atmospheres, hundreds of millions of molecular lines), and maintain the debate alive.

Our group has recently published a series of papers studying the spectrophotometric properties and the star number counts in intermediate age stellar populations (Mouhcine & Lançon 2002; Mouhcine & Lançon 2003; Lançon & Mouhcine 2002; Mouhcine et al. 2002; Mouhcine 2002; hereafter, respectively, Papers I through V). One main purpose of this series was to provide a *global* framework for the study of the various observational aspects of evolved stars in intermediate age populations, ranging from their contribution to the integrated light to the statistical weights of their carbon-rich and oxygen-rich representatives, and also accounting for their contribution to the chemical evolution of a system. We found that our models were successful in reproducing average properties of star clusters as well as of the resolved AGB populations of star fields in Local Group galaxies. The main step forward with these models, when compared to our previous generation of calculations (Lançon et al. 1999), is a more complete inclusion of the physical phenomena governing the evolution through the double-shell burning phase of the AGB, known as the Thermally Pulsing Asymptotic Giant Branch (TP-AGB). From the point of view of stellar population synthesis, two of the most important of these processes are the third dredge-up and envelope burning episodes that can accompany thermal pulses. Only few of the widely used SSP models account for these processes with modern prescriptions. A recent set of complete isochrones was provided by Marigo & Girardi (2001). Because spectrophotometric properties of input library stars are difficult to relate to a precise location on theoretical isochrones (due in particular to pulsation and to the model-dependent nature of the effective temperature definitions of cool stars; see Paper III), we choose to directly provide colours and luminosities of SSPs here.

AGB stars are known to be efficient tracers of intermediate age stellar populations (Menzies et al. 2002; Demers & Battinelli 2002). Their presence in a stellar population leads to red integrated colours, particularly in the near-infrared part of the spectrum where these cool stars emit the bulk of their light. This was highlighted in early observations of star clusters in the Magellanic Clouds (Persson et al. 1983). The inclusion of complex physical processes that strongly affect the evolution through the TP-AGB (envelope burning, the development of a superwind, the “third dredge-up” episodes) has turned out to be crucial to match a variety of observational constraints (see Paper I). The grid presented here provides integrated photometric properties of SSPs calculated for a wide range of ages and initial chemical compositions. It is optimized for studying the near infrared properties of intermediate age stellar populations. We recall that these properties can be strongly affected by stochastic fluctuations when the populations under consideration are small (Lançon & Mouhcine 2000; Bruzual 2002): the values given here refer to the limit of large numbers of stars (in practice, more than  $\sim 10^5$  stars).

The paper is structured as follows. In Sect. 2, we present the input stellar evolution models, and the stellar spectral libraries adopted to convert the theoretical HR diagram into integrated magnitudes and colours. In Sect. 3 we then highlight specific aspects of the predictions that have not been emphasized in the

previous papers of the series. We briefly conclude in Sect. 4. The photometric properties of the SSPs are available in digital form through CDS<sup>1</sup>, or directly from the authors.

## 2. Model description

### 2.1. Stellar evolution

The library of evolutionary tracks used in the population synthesis model from the main sequence to the end of the early-AGB phase is based on the computations of Bressan et al. (1993) and Fagotto et al. (1994a–c). We will refer to these sets as the Padova tracks hereafter.

As we are focusing on the near-infrared properties of intermediate age stellar populations, the accurate inclusion of the latest evolutionary phase of low and intermediate mass stars, through the luminous double-shell burning regime at the end of the AGB, is crucial. We have followed the evolution through this particular phase using an analytical approach known as synthetic evolution modelling (Iben & Truran 1978; Renzini & Voli 1981; Groenewegen & de Jong 1993; Marigo et al. 1996). The model is described in detail in Papers I and II, and the reader is referred to that work for more details. In the following, we simply summarize the basic points. Note that post-AGB phases are not included in the model at this stage. Their contribution to optical and near-infrared fluxes is negligible (Bressan et al. 1994).

The initial conditions for the TP-AGB are taken directly from Padova tracks for different masses and metallicities. The total mass ( $M$ ), core mass, effective temperature ( $T_{\text{eff}}$ ), the luminosity ( $L$ ), and the envelope chemical abundances of the models are then let to evolve according to analytical prescriptions, of which the major ones provide:

1. the core mass-luminosity relation;
2. the core mass-interpulse relation;
3. the core mass evolutionary rate;
4. an approximate effective temperature;
5. the effect of additional CNO burning that may occurs at the bottom of the convective envelope;
6. the instantaneous mass loss rate by stellar winds;
7. the effects of third dredge-up;
8. the composition of the third dredge-up material;
9. the termination of the TP-AGB phase.

The relations (1) and (2) adopted here take into account the effect of metallicity and the envelope burning on the instantaneous luminosity of a star (Wagenhuber & Groenewegen 1998). The inclusion of the third dredge-up process has a significant effect on determining the evolution of the stellar core mass along the TP-AGB, and hence the initial mass-final mass relation. The recurrence of the dredge-up events during this evolutionary phase keeps the core mass close to its value at the beginning of the TP-AGB phase, in agreement with empirical determinations of white dwarf masses. Third dredge-up and envelope burning play a role in the formation of carbon

<sup>1</sup> Centre de Données astrophysiques de Strasbourg, <http://cdsarc.u-strasbg.fr/CDS.html>

stars, which dominate the emission of AGB populations at low metallicity (Frogel et al. 1990).

The final calculations are performed using a mixing length parameter  $\alpha = 2$ , Blöcker's (1995) mass loss prescription ( $\dot{M} = 6.13 \times 10^{-4} \eta L^{4.2} T_{\text{eff}}^{-2} M^{-3.1}$ , with a mass loss efficiency  $\eta = 0.1$ ), dredge-up efficiency  $\lambda = 0.75$ , and the critical core mass to trigger the third dredge-up  $M_c = 0.58 M_{\odot}$ . This set of parameters is shown in Mouhcine & Lançon (2002 a,b) to produce satisfactory agreement with average properties observed in stellar populations of nearby galaxies. The set might not be unique, but it is suitable for further studies of similar statistical properties in other galaxies.

## 2.2. Stellar libraries

Stellar libraries are needed to assign SEDs to the stars of the synthetic populations. For stars evolving through evolutionary phases other than the TP-AGB, we have used the theoretical stellar atmospheres of Kurucz (see Kurucz 1979), Fluks et al. (1994) and Bessell et al. (1989, 1991), as collected and recalibrated by Lejeune et al. (1997, 1998). This library has the advantage of covering a broad range of temperatures, gravities and metallicities.

Most TP-AGB stars are variable. They have cool extended atmospheres in which molecules and dust may form, leading to specific spectral features and SEDs. M type TP-AGB stars display deep water vapour absorption bands. In carbon stars, CN and  $C_2$  absorption bands are dominant and their location in the middle of traditional photometric passbands strongly affects colours. To account for the specific properties of TP-AGB stars, we used the empirical library of average spectra of Paper III.

As discussed in Paper III, the effect of metallicity on the spectra of M type TP-AGB stars is unclear. At low spectral resolution, the shapes of the SEDs of stars in the Large and Small Magellanic Clouds (Lançon & Wood 2000) and near the Galactic Centre (Schultheis et al. 2002) show no striking systematic differences with the shapes observed in the Solar Neighbourhood sample. One tends to find warmer stars at lower metallicities and cooler stars at higher ones, but in this trend it is difficult to disentangle the effects of interior opacities (which determine the evolution of  $T_{\text{eff}}$ ) and of the detailed opacities in the atmospheres (which contribute to determining colours). Red giant atmosphere models indicate that at a given effective temperature ( $T_{\text{eff}}$ ) stars with a higher metal content have redder colours. In the present isochrones, the effect of metallicity on TP-AGB star spectra, at a given effective temperature, is taken into account to first order only, by adopting the metallicity-dependent relation between  $T_{\text{eff}}$  and  $(I - K)$  of Bessell et al. (1991).

## 2.3. Parameters of the isochrone populations

Once the physical parameters of the input databases are defined, the only free parameters of a synthetic SSP are those that describe the initial mass function (IMF).

The IMF can be expressed as:

$$\phi(m) dm = dN/d \log m \propto m^{-(1+x)} dm. \quad (1)$$

The value of the exponent  $x$  is observationally still controversial. For the main tables of this paper we use the standard Salpeter (1955) IMF with  $x = 1.35$ . The adopted lower and upper mass cut-offs are  $M_{\text{min}} = 0.1 M_{\odot}$  and  $M_{\text{max}} = 120 M_{\odot}$ .

The SSP models are single metallicity single burst models where star formation occurs at age 0. The extent of the duration of the initial burst, as long as it does not exceed a few Myr, does not affect the properties of the stellar population at intermediate and old ages.

## 3. Results

The photometric properties of the synthetic SSPs are obtained by convolving their integrated spectra with the response function of each passband. The response functions are taken from Bessell (1990) for the *BVI* photometry and Bessell & Brett (1988) for *JHK* photometry. Vega sets the zero point of all colours. If requested, SSPs can be calculated for other photometric systems.

### 3.1. Colours

Figure 1 shows the time evolution of selected broad-band colours as function of time, for all the SSP metallicities considered.

The figure shows that the colours increase gradually to redder values as the stellar populations age. For  $(V - K)$ , it illustrates that the presence of AGB stars does not immediately translate into a abrupt jump of the integrated colours to the red, but that this transition is smooth (for more detail see Paper I; see also Girardi & Bertelli 1998). This generic behavior of  $(V - K)$  is similar at all metallicities.

Purely near-infrared colours ( $J - H$  and  $H - K$ ) have a particular behavior, especially for metal-poor stellar populations. Indeed those colours increase smoothly up to the age of 0.7–0.8 Gyr, but decrease for older stellar populations up to an age of 1.5–2 Gyr. For older ages the purely near-infrared colours are almost constant over several Gyrs. The short migration of the colours to the red at  $\log(\text{age}) \sim 9.15$  is due to a temporarily enhancement of the AGB star birth rate which occurs as the RGB develops (see Girardi & Bertelli 1998). For stellar populations older than  $\sim 2$  Gyr the changes in colours become very slow. The evolution of near-infrared colours of old stellar populations reflects the sensitivity to the metallicity.

It is instructive to compare the predictions of different models with each other and with data: at intermediate ages, large differences between models exist. We focus on the evolution of  $(V - K)$ , which is strongly sensitive to the contribution of AGB stars both to the *K*-band light and to the bolometric light. Models and data are overlaid in the colour-colour diagram  $(V - K) - (B - V)$ , which is used more and more in the literature for rough age and metallicity estimates of stellar populations (Peletier & Balcells 1996; Puzia et al. 2002; Kissler-Patig et al. 2002).  $(B - V)$  can be taken as the primary age indicator because it is comparatively well understood and not sensitive to the presence of very cool stars.

Systematic differences in  $(V - K)$  of up to  $\sim 0.2$  mag may arise from the colours of the library stars, through the

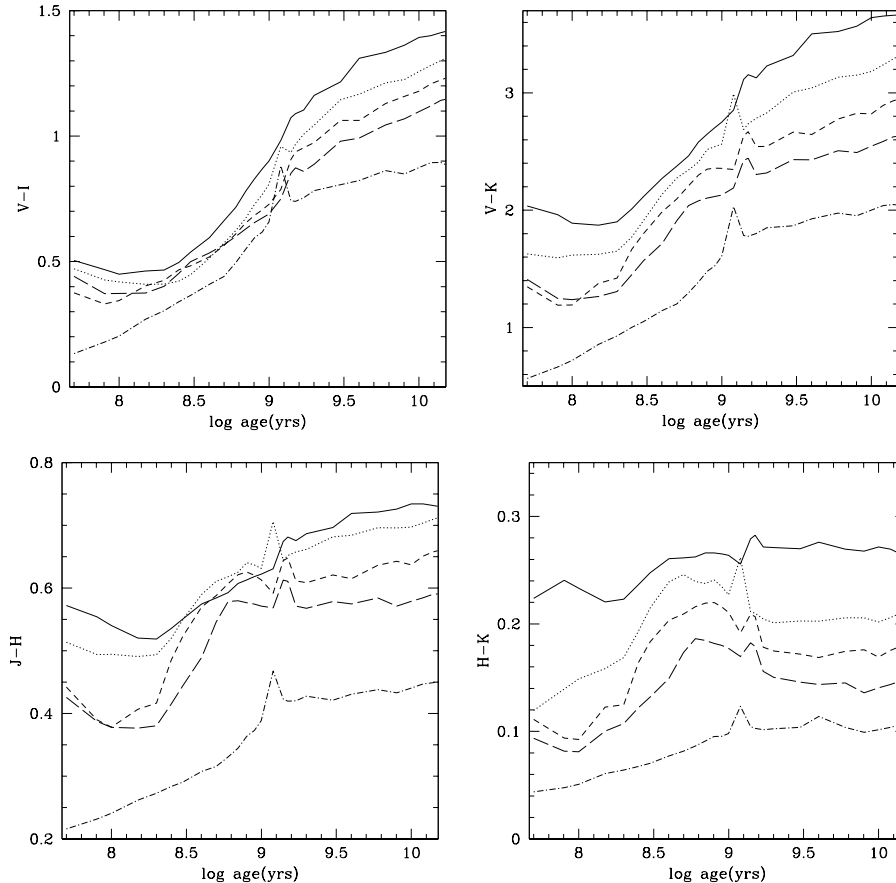


**Fig. 1.** The time evolution of integrated colours ( $V - I$ ), ( $V - K$ ), ( $J - H$ ), and ( $H - K$ ) as a function of age, for the metallicity grid presented in this paper (solid line:  $Z = 0.05$ , dotted:  $Z = 0.02$ , short-dashed:  $Z = 0.008$ , long-dashed:  $Z = 0.004$ , and dot-dashed line:  $Z = 0.0004$ ).

temperature dependence of the  $K$  band bolometric correction,  $BC_K$  and the uncertainties on AGB temperature scales (Lançon & Mouhcine 2002). Models that predict a larger AGB contribution, and thus produce redder values of ( $V - K$ ), will also produce redder near-IR colours as well since AGB stars are the coolest stellar component.  $BC_K$  is similar for carbon stars and O-rich ones, but a stronger relative contribution of carbon stars will lead to a redder value of ( $J - K$ ).

Our predictions for  $Z = 0.02$  and  $Z = 0.008$  are displayed in Fig. 2, together with data for intermediate mass clusters of the LMC and for the massive clusters of NGC 7252 (from Maraston et al. 2001). For comparison, Fig. 3 shows the corresponding plots for the SSP models of Marigo & Girardi (2001, MG01), the latest version of the models of Bruzual & Charlot (BC02)<sup>2</sup>, Maraston (1998, M98), and Fioc & Rocca-Volmerange (1997, FR97). Other models are available in the literature, however they generally use isochrones from one of the above or earlier versions thereof (Vazdekis et al. 1996; Kurt et al. 1999; Schulz et al. 2002), or don't include the TP-AGB evolutionary phase (Leitherer et al. 1999).

The models of FR97 illustrate the abrupt change in ( $V - K$ ) predicted as TP-AGB stars first appear (at ages of  $\sim 100$  Myr) when envelope burning is neglected. Indeed, their TP-AGB

evolution is based on the prescription of Groenewegen & de Jong (1993), which does not account for envelope burning in the luminosity evolution and therefore overestimates the duration of the TP-AGB for stars with initial masses above  $\sim 2.5 M_{\odot}$ . In the other model series (including the one of this paper), the contribution of TP-AGB stars to the light increases progressively, peaking at older ages (0.5–1 Gyr).

In all models but M98, the effect of going from LMC to solar metallicity is to produce slightly redder ( $V - K$ ) colours at a given ( $B - V$ ). The effect is small because of the degeneracy between age and metallicity: when  $Z$  increases, both ( $B - V$ ) and ( $V - K$ ) in general become redder, and the displacement in the two-colour diagram is grossly parallel to the path of evolution. The relative locations of the two curves are marginally significant in view of the many differences in the model inputs. Let us take a few examples. As discussed by Maraston et al. (2001), the TP-AGB contributions to the bolometric light are quasi-identical at the two metallicities in M98, and the colour difference results from the higher efficiency of carbon star formation at lower  $Z$  and from the redder colours adopted for these stars. In our models, the relative contributions of TP-AGB stars to the bolometric luminosity of an SSP is only slightly higher at solar metallicity (Paper I). The metallicity dependence of the efficiency of carbon star formation, though based on different calculations, scale similarly to that of M98. The adopted colours for TP-AGB stars participate in defining the relative

<sup>2</sup> Private communication. See description in Liu et al. (2000).

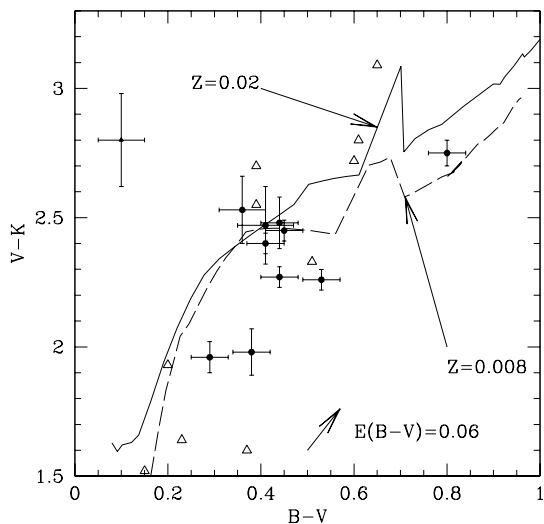


**Fig. 2.**  $V - K$  vs.  $B - V$  two-colour diagram. The solid dots with error bars correspond to the star clusters in the merger remnant NGC 7252 compiled by Maraston et al. (2001). The triangles represent LMC globular clusters with SWB type between 3 and 5.5 (Searle et al. 1980).  $B - V$  comes from van den Bergh (1981) and  $V - K$  from Persson et al. (1983). The typical error bar for LMC clusters is indicated. The lines show the evolution of the SSP models of this paper, for ages ranging from 50 Myr to 15 Gyr.

positions of the tracks (until TP-AGB stars rarely and the red giant properties become dominant, at  $(B - V) \gtrsim 0.8$ ). In the case of MG01, the relative positions of the curves near  $(B - V) = 0.2$  is directly due to the time evolution of  $(B - V)$ , which, in these models, is temporarily redder for the lower  $Z$ .

Neither metallicity, nor uncertainties in the evolution of  $(B - V)$  are sufficient to explain the large differences seen between the predictions of various authors. The colours adopted for the coolest stars play a more important role. The interplay between the physical processes that determine the total amount of light emission during the AGB is crucial. Our models are satisfactorily close to the data, although they tend to lie on the red side of the  $(V - K)$  data points for the younger clusters.

The models of M98 follow the data points well by construction. In those models, the fuel consumption on the TP-AGB phase is set directly to match observed TP-AGB contribution in Magellanic Cloud clusters. This contrasts with the approach of the other groups of authors, who derive TP-AGB contributions from stellar evolution modelling<sup>3</sup>. The models of BC02 and FR97 are bluer in  $(V - K)$  than the data for ages between 0.5 and 1 Gyr, while those of MG01 are systematically too red. In the near future, stochastic simulations will give more insight into the ability of the various models to reproduce the observed dispersion in the data points (Bruzual 2002).

<sup>3</sup> C. Maraston is preparing a new photometric predictions with modified library colours; the trends remain, but redder colours are reached at  $(B - V) = 0.6 - 0.7$ , private communication.

### 3.2. The stellar mass-to-light ratio

The stellar mass-to-light ratio is of crucial importance in studies of the star formation and the dynamical evolution of young and intermediate age populations in starburst and post-starburst galaxies (Smith & Gallagher 2000; Mengel et al. 2001; Silva & Bothun 1998), as well as in the determination of cosmological parameters with galaxies as standard candles (Papovich et al. 2001). Rather than bolometric light, what matters is usually the luminosity in photometric passbands.

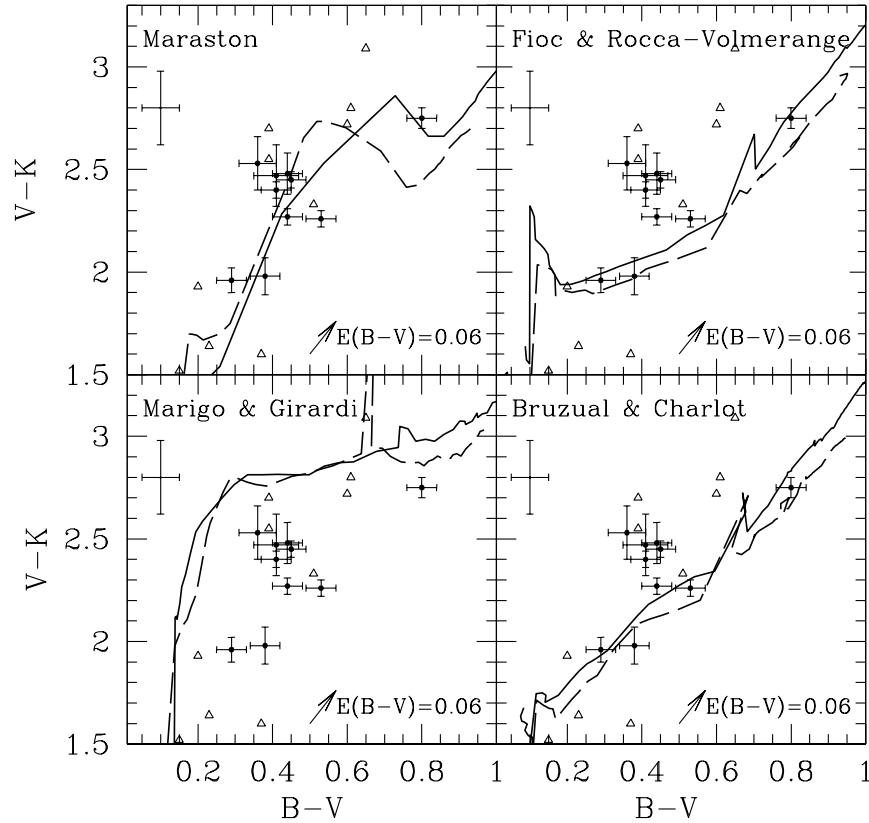
At any age, the stellar population is composed of stars that contribute to the light budget and others that do not. To calculate the total stellar mass, we account for the contributions of both sub-populations. The production rate of dark *stellar remnants* is a function of the stellar population age but also on the adopted IMF. For massive stars we have used metallicity-dependent remnant masses of Portinari et al. (1998). Their estimates have the advantage of accounting for the mass-loss via both stellar winds and supernovae explosions. We have used our synthetic evolution models (see Sect. 2) to estimate the metallicity-dependent remnant masses of low- and intermediate mass stars.

Figure 4 shows the evolution of stellar mass-to-light ratios for the  $V$ -band, the  $K$ -band, and the bolometric light as a function of age for the adopted grid of metallicities. The striking feature in this figure is that the metallicity-dependence of  $M/L_\lambda$  has opposite trends in optical and in near-IR passbands (see also Worthey 1994). The higher the stellar population's metallicity, the higher the  $M/L_\lambda$  ratios for optical passbands, but the lower the near-IR  $M/L_\lambda$  ratios. The wavelength of reversal is near the  $J$ -band, where the effect of metallicity is negligible.

Also worth noting is the flattening of the evolution curve of  $M/L_K$  when the AGB stars appear in the stellar population ( $8.2 \lesssim \log(\text{age}) \lesssim 9.2$ ). When TP-AGB stars are ignored,  $M/L_\lambda$  increases monotonically. The flattening is due to the low effective temperatures of TP-AGB stars. They emit a larger fraction of their bolometric light in the near-infrared than their early AGB progenitors. The evolution of  $M/L_V$  is not affected by the inclusion of TP-AGB in the stellar population.

The mass and the predicted light budget of a stellar population are directly connected to its IMF, but also to the completeness of the stellar evolutionary phases accounted for in the modelling. It is desirable to distinguish between the effects of the IMF and the stellar evolutionary modelling in the evolution of  $M/L_\lambda$  ratios. To this aim, we computed series of models with different IMFs. We considered the descriptions of Miller & Scalo (1979), Kroupa et al. (1993), and a dwarf-dominated IMF ( $x = 1.9$  in Eq. (1)). The same mass cut-offs were kept in all cases ( $M_{\min} = 0.1$ ,  $M_{\max} = 120$ ).

The left panel of Fig. 5 shows the effects of the IMF on  $M/L_K$  and  $M/L_V$  for solar metallicity models. For comparison, the model predictions for the standard Salpeter IMF, with and without TP-AGB stars, are also plotted. The models show that for stellar populations in the age interval between 0.2 Gyr up to 1 Gyr, neglecting TP-AGB stars has an effect equivalent to an increase in the IMF exponent, making the stellar population seem dwarf-dominated. The effect of TP-AGB stars on  $M/L_K$  increases with metallicity.



**Fig. 3.** Similar to Fig. 2 but for different SSP models as indicated in each panel.

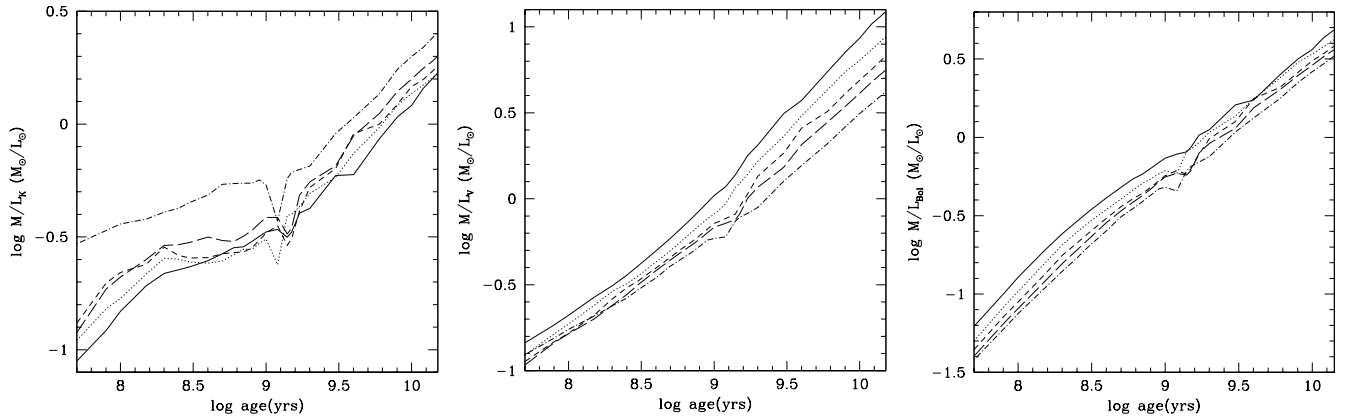


**Fig. 4.** The evolution of stellar mass-to-light ratios for  $K$ -band (left),  $V$ -band (middle) and bolometric light (right). Metallicities are coded with different line styles as in Fig. 1.

#### 4. Summary

In this paper we have presented the photometric properties of new evolutionary synthesis models for SSPs. Those models have been designed with a particular focus on the near-infrared wavelength range and on intermediate ages (0.1–3 Gyr).

To construct these models we have used recent and complete sets of inputs: stellar evolutionary tracks including the late post-main sequence phases that control the evolution of red colours, and stellar libraries accounting for the spectral features of late type stars. Indeed, a particular care was taken to model the contribution of the TP-AGB stars to the total budget of the population light at different wavelength.

A grid of models covering wide ranges in age (from 50 Myr to 15 Gyr) and chemical composition (from  $Z/Z_{\odot} = 1/50$  to  $Z/Z_{\odot} = 2.5$ ) has been constructed and submitted to observational test (Papers I, II and IV). When compared with other recent models in the literature, it provides one of the most satisfactory agreements with the empirical  $(B-V)$ – $(V-K)$  colours available for star clusters.

*Acknowledgements.* We are grateful to C. Maraston and S. Charlot for providing us with their models in electronic form. We would like to thank warmly different colleagues and friends, M. Fioç, M. A. T. Groenewegen, C. Leitherer, D. Silva, J.-L. Vergely, for highlighting discussions. We thank the anonymous referee for a careful reading and for requests that improved the paper.

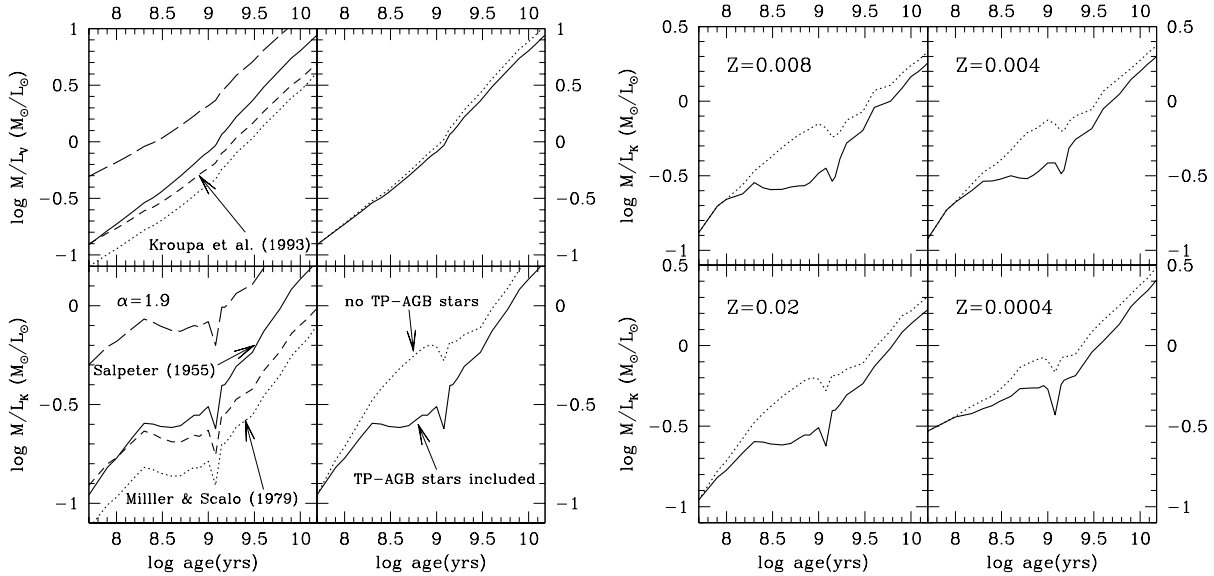


**Fig. 5.** *Left:* effects of the IMF on  $M/L_K$   $M/L_V$  compared to the effect of TP-AGB stars, at solar metallicity. *Right:* effect of TP-AGB stars on the  $K$ -band mass-to-light ratio for different metallicities as noted in the plots. Continuous lines show models where TP-AGB stars are accounted for, while dotted lines show models where these stars are neglected.

## References

- Arimoto, N., & Yoshii, Y. 1987, *A&A*, 188, 23  
 Bertelli, G., Bressan, A., Chiosi, C., Fagotto, F., & Nasi, E. 1994, *A&AS*, 106, 275  
 Bessell, M. S., & Brett, J. M. 1988, *PASP*, 100, 1134  
 Bessell, M. S., Brett, J. M., Scholz, M., & Wood, P. R. 1989, *A&AS*, 77, 1  
 Bessell, M. S. 1990, *PASP*, 102, 1181  
 Bessell, M. S., Brett, J. M., Scholz, M., & Wood, P. R. 1991, *A&AS*, 89, 335  
 Blöcker, T. 1995, *A&A*, 297, 727  
 Bressan, A., Fagotto, F., Bertelli, G., & Chiosi, C. 1993, *A&AS*, 100, 647  
 Bressan, A., Chiosi, C., & Fagotto, F. 1994, *ApJS*, 94, 63  
 Bruzual, A. G. 1983, *ApJ*, 273, 105  
 Bruzual, A. G., & Charlot, S. 1993, *ApJ*, 405, 538  
 Bruzual, A. G. 2002, in *Proc. IAU Symp. 207, Extragalactic Star Clusters*, in press  
 Charlot, S., & Bruzual, A. G. 1991, *ApJ*, 367, 126  
 Demers, S., & Battinelli, P. 2002, *AJ*, 123, 238  
 Fagotto, F., Bressan, A., Bertelli, G., & Chiosi, C. 1994a, *A&AS*, 104, 365  
 Fagotto, F., Bressan, A., Bertelli, G., & Chiosi, C. 1994b, *A&AS*, 105, 29  
 Fagotto, F., Bressan, A., Bertelli, G., & Chiosi, C. 1994c, *A&AS*, 105, 39  
 Fioc, M., & Rocca-Volmerange, B. 1997, *A&A*, 326, 950  
 Fluks, M. A., Plez, B., Thé, P. S., et al. 1994, *A&AS*, 105, 311  
 Forbes, D. A., Masters, K. L., Minniti, D., & Barmby P. 2000, *A&A*, 358, 471  
 Frogel, J. A., Mould, J., & Blanco, V. M. 1990, *ApJ*, 352, 96  
 Girardi, L., & Bertelli, G. 1998, *MNRAS*, 300, 533  
 Girardi, L., Bressan, A., Bertelli, G., & Chiosi, C. 2000, *A&AS*, 141, 371  
 Groenewegen, M., & de Jong, T. 1993, *A&A*, 267, 410  
 Groenewegen, M., van den Hoek, L. B., & de Jong, T. 1995, *A&A*, 293, 381  
 Iben, I., & Truran, J. W. 1978, *ApJ*, 220, 980  
 Kissler-Patig, M., Brodie, J. P., & Minniti, D. 2002, *A&A*, 391, 441  
 Kroupa, P., Tout, C. A., & Gilmore, G. 1993, *MNRAS*, 262, 545  
 Kurth, O. M., Fritze-v. Alvensleben, U., & Fricke, K. J. 1999, *A&AS*, 138, 19  
 Kurucz, R. L. 1979, *ApJS*, 40, 1  
 Lançon, A., & Mouhcine, M. 2000, in *Massive Stellar Clusters*, ed. A. Lançon, & C. M. Boily, *ASP Conf. Ser.*, 211, 34  
 Lançon, A., & Mouhcine, M. 2002, *A&A*, 393, 167 (Paper III)  
 Lançon, A., & Rocca-Volmerange 1996, *New Astron.*, 1, 215  
 Lançon, A., & Wood, P. R. 2000, *A&AS*, 146, 217  
 Lançon, A., Mouhcine, M., Fioc, M., & Silva, D. 1999, *A&A*, 344, L21  
 Leitherer, C., Schaerer, D., Goldader, J., et al. 1999, *ApJS*, 123, 3  
 Lejeune, T., Cuisinier, F., & Buser, R. 1997, *A&AS*, 125, 229  
 Lejeune, T., Cuisinier, F., & Buser, R. 1998, *A&AS*, 130, 65  
 Liu, M. C., Charlot, S., & Graham, J. R. 2000, *ApJ*, 543, 644  
 Maraston, C. 1998, *MNRAS*, 300, 872  
 Maraston, C., Kissler-Patig, M., Brodie, J. P., Barmby, P., & Huchra, J. P. 2001, *A&A*, 370, 176  
 Marigo, P., Bressan, A., & Chiosi, C. 1996, *A&A*, 313, 545  
 Marigo, P., Girardi, L. 2001, *A&A*, 377, 132  
 Mengel, S., Lehnert, M. D., Thatte, N., Tacconi-Garman, L. E., & Genzel, R. 2001, *ApJ*, 550, 280  
 Menzies, J., Feast, M., Tanabe, T., Whitelock, P., & Nakada, Y. 2002, *MNRAS*, 335, 923  
 Miller, G. E., & Scalo, J. M. 1979, *ApJS*, 41, 513  
 Mouhcine, M., & Lançon, A. 2002a, *A&A*, 393, 149 (Paper I)  
 Mouhcine, M., & Lançon, A. 2003, *MNRAS*, 338, 572 (Paper II)  
 Mouhcine, M. 2002, *A&A*, 394, 125 (Paper V)  
 Mouhcine, M., Lançon, A., Leitherer, C., Silva, D., & Groenewegen, M. A. T. 2002, *A&A*, 393, 101 (Paper IV)  
 Papovich, C., Dickinson, M., & Ferguson, H. C. 2001, *ApJ*, 559, 620  
 Peletier, R. F., & Balcells, M. 1996, *AJ*, 111, 2238  
 Persson, S. E., Aaronson, M., Cohen, J. G., Frogel, J. A., & Matthews, K. 1983, *ApJ*, 266, 105  
 Portinari, L., Chiosi, C., & Bressan, A. 1998, *A&A*, 334, 505

- Puzia, T. H., Zepf, S. E., Kissler-Patig, M., et al. 2002, *A&A*, 391, 453  
Renzini, A., & Voli, M. 1981, *A&A*, 94, 175  
Salpeter, E. E. 1955, *ApJ*, 121, 161  
Schultheis, M., Lançon, A., Omont, A., Schuller, F., & Ohja, D. K. 2002, in preparation  
Schweizer, F., Miller, B. W., Whitmore, B. C., & Fall, S. M. 1996, *ApJ*, 112, 1839  
Searle, L., Wilkinson, A., & Bagnuolo, W. G. 1980, *ApJ*, 239, 803  
Silva, D. R., & Bothun, G. D. 1998, *AJ*, 116, 85  
Tinsley, B. M. 1980, *Fund. Cosmic Phys.*, 5, 287  
Smith, L. J., & Gallagher, J. S. 2000, *MNRAS*, 326, 1027  
van den Bergh, S. 1981, *A&AS*, 46, 79  
Vassiliadis, E., & Wood, P. R. 1993, *ApJ*, 413, 641  
Wagenhuber, J., & Groenewegen, M. A. T. 1998, *A&A*, 340, 183  
Whitmore, B. C., Schweizer, F., Kundu, A., & Miller, B. W. 2002, *AJ*, 124, 147  
Worthey, G. 1994, *ApJS*, 95, 107  
Zepf, S. E., & Ashman, K. E. 1993, *MNRAS*, 264, 611